Topology Optimization of an Actively Cooled Electronics Section for Downhole Tools

S. Soprani*[1], J. H. K. Haertel[1], B. S. Lazarov[2], O. Sigmund[2], K. Engelbrecht[1],
[1] Department of Energy Conversion and Storage - Technical University of Denmark, [2]Department of Mechanical Engineering - Technical University of Denmark.
* Frederiksborgvej 399 - Building 778, 4000 Roskilde, Denmark, stefs@dtu.dk

Abstract: Active cooling systems represent a possible solution to the electronics overheating that occurs in wireline downhole tools operating in high temperature oil and gas wells. A Peltier cooler was chosen to maintain the downhole electronics to a tolerable temperature, but its integration into the downhole electronics unit proved to be challenging, because of the space constraints and the proximity of the cooling zone (electronics) to the heat sink (well fluid). The topology optimization approach was therefore chosen to optimize the thermal design of the actively cooled electronics section and the SIMP (Solid Isotropic Material with Penalization) method was implemented in COMSOL Multiphysics. Several optimized designs were obtained for different operating conditions and their sensitivity to the change in the boundary conditions was evaluated. A final design for the electronics unit was selected, according to the topology optimization results and assembly constraints, and compared to the optimized cases.

Keywords: Topology optimization, SIMP, Electronics cooling.

1. Introduction

Well interventions are remedial operations that are performed in oil and gas wells in order to restore or increase the production. The *electric wireline* well intervention technique relies on the usage of a cabling technology that connects the downhole tools to the surface equipment and, thanks to the integration of electronic components into the downhole devices, allows the operator to remotely control the tool during the operation. However, the application of the wireline technique in high temperature wells, where the temperature can range between 150 °C and 200 °C, is often restricted by the electronics temperature limit, which is currently set to 175 °C for the majority of the employed components available on the market.

Active cooling systems represent a possible solution to the electronics overheating [1] as they could extend the application of the wireline tools to a wider range of high temperature wells. The high-temperature sensitive electronics would be maintained below the well temperature, while the well fluid would be used as a heat sink for the cooler excessive heat. A thermoelectric cooler (TEC) was chosen to fulfill this task [2], because of its compactness and lack of moving parts; on the other hand its low efficiency (COP) might generate issues due to excessive heat rejection at the hot end in the case of low convection regimes in the oil well.. It is therefore very important to define an effective thermal design of the electronics unit that provides a good thermal path to reject the excessive heat to the well, protects the cooled electronics from the hot surroundings and minimizes the heat leakages. The limited availability of space in the downhole tool and the proximity between the cooling load and the heat sink make this task challenging.

The topology optimization approach was adopted in order to define an optimized distribution of the thermal conductive material and thermal insulation, so the high-temperature sensitive components' temperature could be minimized. The geometry of the electronics unit was modelled in COMSOL Multiphysics and the topology optimization SIMP (Solid Isotropic Material with Penalization) method [3] was implemented. A density filter was applied in order to avoid mesh-dependent solutions, and coupled with a projection function, in order to obtain a better resolution of the design variable distribution that defines the optimized distribution of thermally conductive material and thermal insulation.

2. System integration overview

The downhole tool electronics unit (Figure 1) is composed of two main structural components: a 200 mm long cylindrical *chassis* (O.D. 60 mm), on which the electronic components are installed,

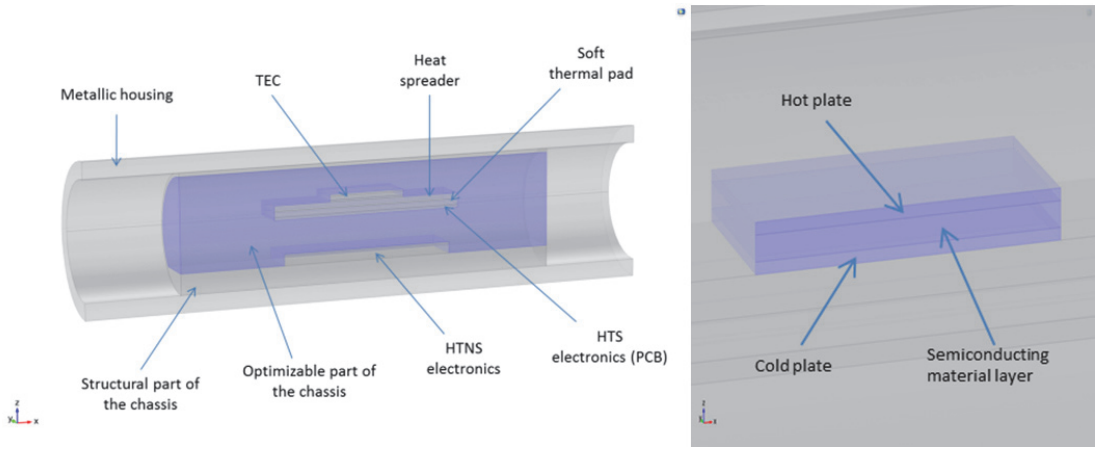

Figure 1. COMSOL Multiphysics representation of the longitudinal section of the downhole tool (left side) and particular of the TEC device with the two plates and the semiconducting material layer highlighted in blue (right side).

and a 300 mm long metallic *housing* (O.D. 80 mm, I.D. 60 mm), which encloses the chassis and the electronics, protecting and sealing them from the outer well fluid at high pressure. The chassis, in turn, is divided into a "*structural*" part made of aluminum, that provides mechanical stability to the system, and an "*optimizable*" part, that will be the object of the topology optimization.

Furthermore, the electronic components can be distinguished into *high temperature-non sensitive (HTNS)* and *high temperature-sensitive (HTS)* components. The first dissipate 5 W, are mounted directly on the chassis and are passively cooled; the latter dissipate 1 W, are installed on a printed circuit board (PCB) and are actively cooled with the TEC. The TEC cold plate is thermally coupled with the HTS electronics through a copper *heat spreader* and a *soft thermal pad*. On the other side, the TEC hot plate needs to be thermally connected to the well fluid through a heat sink that the topology optimization solver is asked to optimize. The design of the system aims at maintaining the HTS electronics below 175 °C, when operating in a 200 °C well environment.

3. Governing equations

The heat transfer within the system is mainly driven by heat conduction, so the heat transfer PDE (Eq. 1) was implemented in the COMSOL model through the Heat Transfer module.

$$\nabla(-k\nabla T) = Q_{source} \tag{1}$$

Where k ($Wm^{-1}K^{-1}$) is the material thermal conductivity, T (K) is the temperature and Q_{source} (Wm^{-3}) is a volumetric heat source.

A modified heat transfer equation, that accounted for the thermoelectric effect, was implemented in the TEC semiconductor domain, in between the TEC hot and cold plates, through the Coefficient Form PDE module.

$$\nabla(\boldsymbol{J}ST - k\nabla T) = Q_{JouleHeating} \tag{2}$$

Where $\boldsymbol{J}$ (Am^{-2}) is the electric current density vector, S (VK^{-1}) is the material Seebeck coefficient, $Q_{JouleHeating}$ (Wm^{-3}) is the heat source associated to the Joule effect. The layer between the TEC hot and cold plates (Figure 1), in reality, is composed of leg pairs of semiconductor material (Bi_2Te_3) separated by air; in order to reduce the geometry complexity this layer was modelled as isotropic and homogeneous, and its properties were weighted based on the volumes of Bi_2Te_3 and air (Eq. 3, 4, 5). Equations from Gordon et al. [4] were used to characterize the behavior of Bi_2Te_3, while the COMSOL material library was used for the air properties. The equations were combined through linear coefficients in order to match a commercial Peltier cooler performance that was evaluated in terms of hot and cold plate temperatures at different cooling loads and operating temperatures.

$$S = S_1(-2.025e-9T^2 + 1.42e-6T + \\ -4.49e-5) \tag{3}$$

$$k = k_1(2.91e-5T^2 - 0.019T + 4.81) + \\ +k_2\, k_{air}(T) \tag{4}$$

$$\sigma = \sigma_1(4.35e.8T - 2.754e - 6)^{-1} \quad (5)$$

$$Q_{JouleHeating} = 0.268\,\sigma^{-1}\boldsymbol{J}\cdot\boldsymbol{J} \quad (6)$$

Where $k_{air}(T)$ ($Wm^{-1}K^{-1}$) is the thermal conductivity of air as a function of temperature from the COMSOL material library; S_1 = 0.349, k_1 = 0.215, k_2=0.732 and σ_1 = 0.309 are linear coefficients. At the two ends of the electronics unit, an adiabatic boundary condition was set. A convective heat flux, simulating the well fluid interaction with the housing surface, was imposed by setting the external well fluid temperature T_{fl} and heat transfer convective coefficient h. The partial differential equations (1) and (2) were then interfaced through a Dirichlet boundary condition that matched the temperatures at the interface. Heat sources were set in the HTNS electronics domain (5W) and at the interface between the PCB and the soft thermal pad (1 W), to simulate the electronics power dissipation. According to empirical estimations, thermal contact resistances were simulated by setting a thin resistive layer at the interface between the structural chassis and the housing (R_{th1} = 1.1e-3 m^2KW^{-1}), between the HTNS electronics and the structural chassis (R_{th2} = 2.5e-5 m^2KW^{-1}), and between the TEC plates and the structural chassis/heat spreader (R_{th3} = 2.5e-5 m^2KW^{-1}). R_{th1} was estimated through the comparison between simulation results and experimental data from thermal tests on the structural chassis. R_{th2} and R_{th3} instead, simulated a 0.1 mm thick layer of thermal grease, with a thermal conductivity of 4 $Wm^{-1}K^{-1}$. Another relevant boundary condition was set for the TEC feed current I_{feed} and used to characterize the cooler operating state.

4. Topology optimization implementation

The topology optimization problem can be stated as follows:

$$minimize: \quad f_{obj}(T, \rho_{design}) = \frac{1}{A_{PCB}}\int_{\Omega_{PCB}} T\, d\Omega_{PCB} \quad (7)$$

$$constraints: \quad 0 \le \rho_{design} \le 1 \quad (8)$$

$$0 \le \int_{\Omega} \rho_{design} d\Omega \le \gamma V_{\Omega} \quad (9)$$

$$0 \le \gamma \le 1 \quad (10)$$

$$\boldsymbol{r}(T, \rho_{design}) = \boldsymbol{0} \quad (11)$$

Where f_{obj} is the objective function to be minimized, defined as the integral average of the temperature distribution along the PCB surface Ω_{PCB}; A_{PCB} is the PCB area surface (m^2), ρ_{design} is the design variable that can range between 0 (thermal insulation) and 1 (aluminum), and whose distribution needs to be optimized; γ is the fraction of the optimizable domain V_{Ω} that sets the constraint on the maximum volume that can be occupied by aluminum; $\boldsymbol{r}(T, \rho_{design})$ is the residual of the discretized system of the state equations reported in section 3.

The topology optimization problem was implemented in COMSOL through the Optimization module: ρ_{design} was defined and bounded as a *control variable field*, while the volume constraint was set with an *integral inequality constraint*. A density filter [5] was applied to the design variable, in order to make the solution independent from the mesh size (Eq. 12), and implemented in COMSOL through the Coefficient Form PDE module:

$$-r^2\nabla^2\tilde{\rho} + \tilde{\rho} = \rho_{design} \quad (12)$$

Where r is a filter parameter and is equal to 1.5 times the maximum mesh element length in the optimizable domain. $\tilde{\rho}$ was then projected in order to obtain a sharper transition zone between aluminum and insulator in the optimized topology [6]; Eq. 13 was used.

$$\bar{\tilde{\rho}} = \frac{tanh(\beta\eta) + tanh(\beta(\tilde{\rho} - \eta))}{tanh(\beta\eta) + tanh(\beta(1 - \eta))} \quad (13)$$

η = 0.5 ensured a good convergence of the solution; β was ramped from 1 to 8, using the continuation approach, as suggested by Wang et al. [7]. The thermal properties of the optimizable domain were then calculated through the projected design variable, with an interpolation function that defined the thermal conductivity.

$$k_{\Omega} = k_{ins} + (k_{Al} - k_{ins})\bar{\tilde{\rho}}^{p} \quad (14)$$

Where k_{Ω} ($Wm^{-1}K^{-1}$) is the domain effective thermal conductivity, k_{ins} = 0.17 $Wm^{-1}K^{-1}$ and k_{Al}= 138 $Wm^{-1}K^{-1}$ are respectively the thermal conductivities of the thermal insulation and of the considered aluminum alloy, and p = 3 [7] is the penalization coefficient.

The problem was solved through the optimization solver MMA (Method of Moving Asymptotes), embedded in COMSOL.

5. Results

The model was simulated for a well temperature of 200 °C and different conditions of well fluid convection regimes h and TEC feed current I_{feed}, so the design could be optimized for different operating conditions.

The system was optimized for I_{feed} of 1, 2, 3 and 4 A, according to the modelled commercial cooler specifications, and for h of 25, 50, 100 and 500 $Wm^{-2}K^{-1}$, in order to reproduce low, medium-low and medium well fluid convection regimes. h = 25 $Wm^{-2}K^{-1}$ is defined as the worst case design condition, while for h > 500 $Wm^{-2}K^{-1}$ the design of the unit is expected not to be critical anymore. The optimization of the system balanced the use of aluminum and thermal insulation in different ways at different boundary conditions; a tradeoff between thermal protection of the cooled electronics and heat rejection of the excessive heat was always reached and two main design concepts were individuated.

Low TEC feed currents and high values of convective coefficients led to an optimized design (*Design 1*) where an aluminum pad connects the cooler hot plate to the structural chassis, so the excessive heat can be rejected radially through the housing to the well (Figure 2). Low I_{feed} (low ohmic losses across the cooler) and high h values make the heat rejection process not critical, so the thermal protection of the cooled electronics is prioritized and the use of aluminum is limited to provide a radial heat sink. The length of the aluminum pad increases when the feed current grows or the heat transfer convective coefficient decreases.

High TEC feed currents and low values of convective coefficients, on the other side, led to a design (*Design 2*) where the heat rejection becomes more problematic than in the previous case. An aluminum layer is now attached to the structural chassis (Figure 3). This layer does not only provide a radial path for the excessive heat to be rejected to the well, but also spreads it along the longitudinal direction of the tool; a better distribution of the heat enhances the heat exchange with the well fluid and minimizes the heat backflow to the cooled electronics. Thermal insulation still protects the cooled electronics from the HTNS components and the hot surroundings. The thickness of the layer increases with I_{feed} and when h decreases.

The balance between materials can be evaluated, for different boundary conditions, through the ratio of used aluminum over the optimizable volume (Figure 4).

$$R = \frac{1}{V_\Omega}\int_\Omega \bar{\tilde{\rho}}\, d\Omega \qquad (15)$$

Where R is the aluminum usage ratio and V_Ω is the optimizable domain volume (m^3). In order to have a good overview of the system behavior, the sensitivity of the optimized designs to operations at different boundary conditions was assessed. The performance of the system was evaluated in terms of temperature at which the HTS electronics could be maintained.

The electronics section was initially optimized for a certain value of feed current and well fluid convective coefficient; the resulting

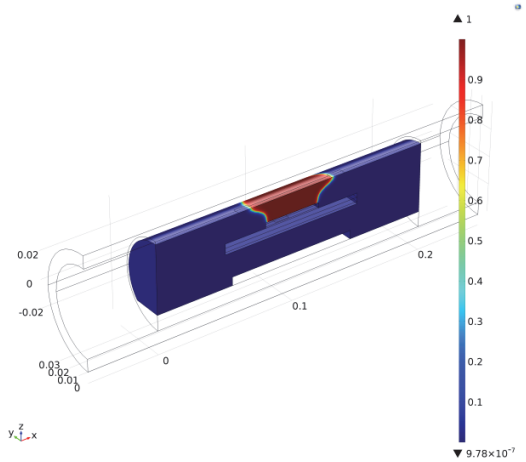

Figure 2. $\bar{\tilde{\rho}}$ distribution for the *Design 1* concept. System optimized for I_{feed} = 1 A and h = 100 $Wm^{-2}K^{-1}$.

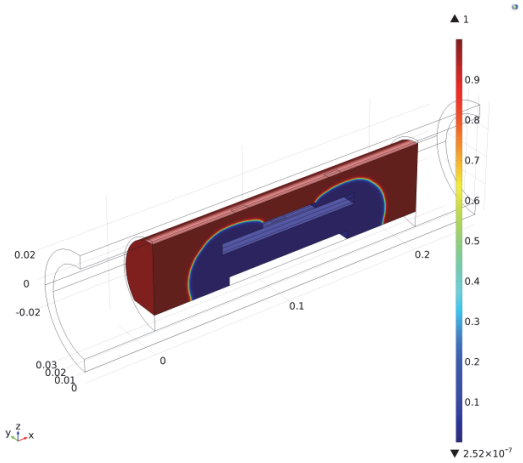

Figure 3. $\bar{\tilde{\rho}}$ distribution for the *Design 2* concept. System optimized for I_{feed} = 4 A and h = 50 $Wm^{-2}K^{-1}$.

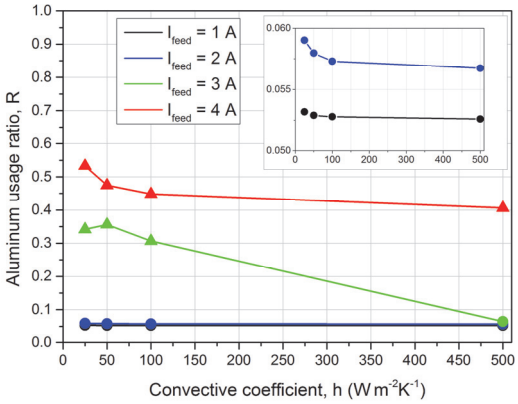

Figure 4. *R* vs. well fluid convective coefficient, for different TEC feed currents. Different symbols refer to the different optimized design concepts.
● = Design 1, ▲ = Design 2.

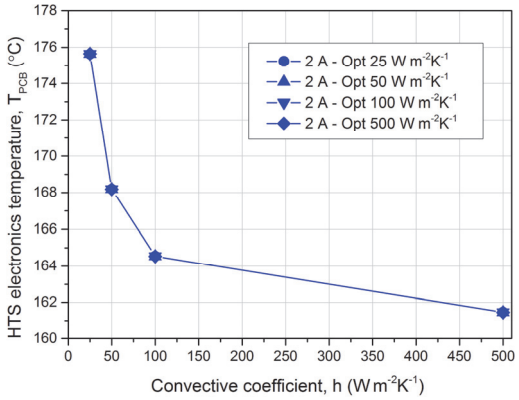

Figure 5. HTS electronics temperature vs. well fluid convective coefficient for four different systems, optimized for I_{feed} = 2 A and h = 25, 50, 100 and 500 $Wm^{-2}K^{-1}$.

design was then simulated, maintaining the TEC feed current constant, at different values of well fluid convective coefficients. Figure 5 reports the performance of the optimized designs versus the well fluid convective coefficient: each of the five illustrated curves refers to a system optimized for I_{feed} = 2 A and a different value of h. It can be noticed the five curves overlap and the performance of the systems is very similar, despite they were optimized for different h values. A maximum temperature mismatch of 0.05 °C between the curves was found. The same behavior was obtained with the optimizations with the other feed currents. For I_{feed} = 1 A the maximum mismatch between the curves is equal to 0.005 °C, for I_{feed} = 3 A is equal to 0.88 °C and for I_{feed} = 4 A is equal to 0.88 °C. We can conclude the optimization of the electronics unit, at a given feed current is not significantly sensitive to the well fluid convective coefficients in the considered range; in other words, the performance of the optimized systems, at a given feed current, is not significantly sensitive to the length/thickness of the optimized aluminum pad/layer and can be considered robust.

The same approach was used to evaluate the sensitivity of the optimized designs to the TEC feed current, at a given convective coefficient. The electronics section was first optimized for a certain value of feed current and well fluid convection; the resulting design was then simulated, maintaining the convection regime constant, at different values of operating current. Figure 6 shows the optimization process is more sensitive to the feed current as the mismatch between the curves can go up to several degrees Celsius. An optimal feed current I_{opt} that minimizes the HTS electronics temperature can be individuated. It can be defined as the TEC feed current at which the marginal gain in absorbed heat flux, due to an infinitesimal increase of the TEC feed current, becomes lower than the heat flux that leaks through the insulation. I_{opt} is slightly different for each optimized design, but mainly depends on h and on the well fluid capability of absorbing the excessive heat. I_{opt} is equal to ~1.9 A for h = 25 $Wm^{-2}K^{-1}$, to ~2.3 A for h = 50 $Wm^{-2}K^{-1}$, to ~2.6 A for h = 100 $Wm^{-2}K^{-1}$ and to ~2.9 A for h = 500 $Wm^{-2}K^{-1}$. The designs that best operate around the optimal current are the ones optimized for 2 A and 3 A.

The topology optimization results, together with the knowledge of the practical assembly constraints, were used to define the final design for the actively cooled downhole electronics unit (Figure 7). *Design 1* proved to be as well performing as *Design 2* around the optimal current, but with a lower employment of aluminum and therefore with a lower weight. The aluminum pad that provided the thermal path from the cooler hot plate to the structural chassis proved to be crucial. An aluminum pad, 41x41 mm was therefore implemented in the final design, illustrated in Figure 7. No aluminum layer was included, except for 2 walls, 10 mm thick, at each end of the chassis. They provide mechanical stability, an additional

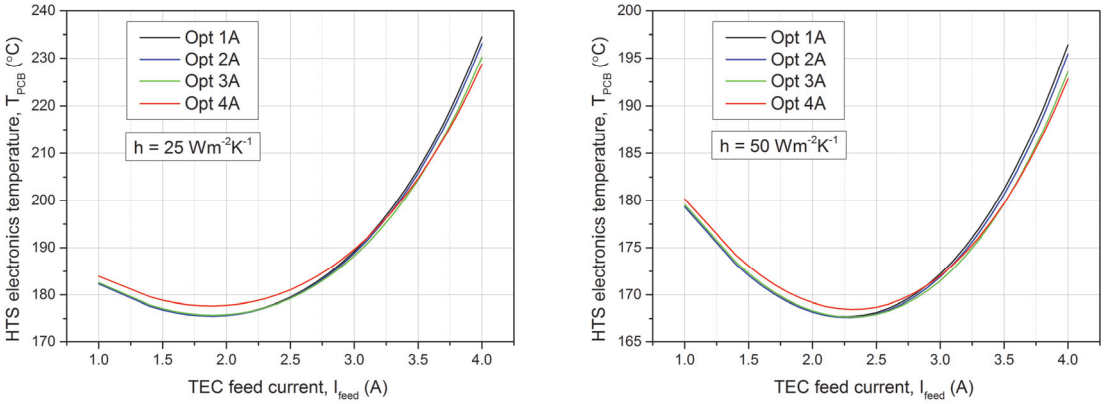

Figure 6. HTS electronics temperature vs. TEC feed current for four different systems, optimized for I_{feed} = 1, 2, 3 and 4 A, and h = 25 $Wm^{-2}K^{-1}$ (left side) and 50 $Wm^{-2}K^{-1}$ (right side).

thermal path for the heat to better spread in case of low heat rejection rate, and are suitable for the installation of pins for the assembly of the system. The chassis would be in fact split in a bottom half, were the HTNS electronics are installed, and a top half, where the cooling system is installed. The two halves would then be coupled and held in place by four pins (not reported in Figure 7). Two smaller pads, 8x8 mm, with threaded holes, were also designed in the top part of the chassis in order to clamp the cooler in between the heat spreader and the chassis itself, through a plastic screw system. The rest of the domain is filled with thermal insulation.

Simulations proved the chosen design operates very closely to the optimized systems performance (Table 1). The difference in HTS electronics temperature is very small when operating at 1 or 2 A, as the chosen design is very similar to the *Design 1* concept: the electronics is maintained maximum 0.09 K above the HTS electronics temperature in the optimized case. When operating at 3 and 4 A the mismatch becomes higher, since the *Design 2* concept would work better at high feed currents. However, the HTS components are always maintained less than 1 K above the optimized case for operations at 3 A. The mismatches are larger than 1 K for I_{feed} = 4 A, but can be

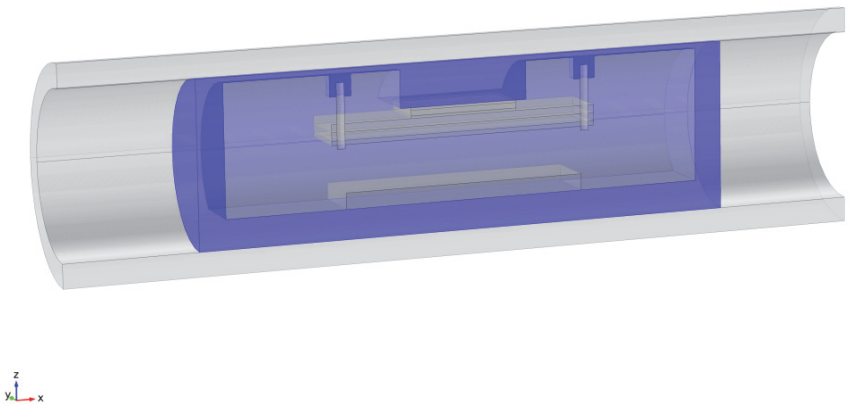

Figure 7. COMSOL Multiphysics illustration of the longitudinal section of the final design. The designed aluminum chassis is highlighted in blue.

considered irrelevant; a feed current of 4 A is far from the observed optimal feed currents and the system would always aim to operate close to the optimal conditions, between 2 and 3 A.

Table 1. Comparison between the performance of the optimized systems (Opt) and final chosen design (Design). $\Delta T = T_{HTS,design} - T_{HTS,Opt}$.

h $(Wm^{-2}K^{-1})$	*Opt - 1A* T_{HTS} *(°C)*	*Design - 1A* T_{HTS} *(°C)*	ΔT *(K)*
25	182.31	181.95	0.10
50	179.32	178.97	0.11
100	177.83	177.47	0.11
500	176.56	176.21	0.11
h $(Wm^{-2}K^{-1})$	*Opt - 2A* T_{HTS} *(°C)*	*Design - 2A* T_{HTS} *(°C)*	ΔT *(K)*
25	175.63	175.68	0.05
50	168.18	168.23	0.05
100	164.54	164.57	0.04
500	161.46	161.48	0.03
h $(Wm^{-2}K^{-1})$	*Opt - 3A* T_{HTS} *(°C)*	*Design - 3A* T_{HTS} *(°C)*	ΔT *(K)*
25	188.22	188.93	0.71
50	171.48	171.87	0.39
100	163.68	163.90	0.22
500	157.12	157.35	0.23
h $(Wm^{-2}K^{-1})$	*Opt - 4A* T_{HTS} *(°C)*	*Design - 4A* T_{HTS} *(°C)*	ΔT *(K)*
25	228.62	233.59	4.97
50	192.79	195.71	2.92
100	177.25	179.29	2.04
500	165.23	166.37	1.14

6. Conclusions

The distribution of thermally conductive material and thermal insulation was optimized within an actively cooled electronics unit for downhole tools. The heat transfer mechanisms were modelled in COMSOL Multiphysics and the topology optimization SIMP method was implemented. Diverse design concepts were obtained for different boundary conditions. The analysis of the resulting designs supported the development of a final unit, whose performance was compared to the optimized cases. An acceptable deviation between them was assessed and the importance of controlling the operating conditions close to the optimal TEC feed current was underlined.

7. Acknowledgments

S. Soprani and K. Engelbrecht would like to show their gratitude to the Danish Ministry of Technology and Innovation and to Welltec A/S for partially funding this work. The authors would also like to acknowledge the TopTEN project, sponsored through the Sapere Aude Program of the Danish Council for Independent Research (DFF–4005-00320), for supporting this study.

8. References

[1] A.G. Flores. Active Cooling for Electronics in a Wireline Oil-Exploration Tool, *Ph.D. thesis*, M.I.T., USA (1996).

[2] S. Soprani, K. Engelbrecht, A.J. Nørgaard. Active Cooling and Thermal Management of a Downhole Tool Electronics Section, *Proceedings of the 24th IIR International Congress of Refrigeration*, Yokohama, Japan (2015).

[3] E.M. Dede, J. Lee, T. Nomura. Multiphysics simulation: electromechanical system applications and optimization, *Springer London* (2014).

[4] J.M. Gordon, K.C. Ngc, H.T. Chuac, A. Chakrabortyc, The electro-adsorption chiller: a miniaturized cooling cycle with applications to micro-electronics, *International Journal of Refrigeration,* 25 (8): 1025–1033 (2002).

[5] B. S. Lazarov, O. Sigmund. Filters in Topology Optimization Based on Helmholtz-Type Differential Equations, *International Journal for Numerical Methods in Engineering*, 86 (6): 765-781 (2011).

[6] F. Wang, B. S. Lazarov, O. Sigmund. On Projection Methods, Convergence and Robust Formulations in Topology Optimization, *Structural and Multidisciplinary Optimization*, 43 (6): 767-784 (2011).

[7] O. Sigmund, K. Maute. Topology Optimization Approaches, *Structural and Multidisciplinary Optimization*, 48 (6): 1031-1055 (2013).